Bioresource Technology 270 (2018) 46–54

Contents lists available at ScienceDirect

Bioresource Technology

journal homepage: www.elsevier.com/locate/biortech

Inhibition of anammox by sludge thermal hydrolysis and metagenomic insights

Zaoli Gu[a,b,1], Yuan Li[b,c,1], Yifeng Yang[a,b], Siqing Xia[a,d,*], Slawomir W. Hermanowicz[b,c], Lisa Alvarez-Cohen[a,b]

[a] State Key Laboratory of Pollution Control and Resource Reuse, College of Environmental Science and Engineering, Tongji University, 1239 Siping Road, Shanghai 200092, China
[b] Department of Civil and Environmental Engineering, University of California, Berkeley, CA 94720, USA
[c] Tsinghua-Berkeley Shenzhen Institute, University of California, Berkeley, CA 94720, USA
[d] Shanghai Institute of Pollution Control and Ecological Security, 1239 Siping Road, Shanghai 200092, China

ARTICLE INFO

Keywords:
Thermal hydrolysis pre-treated sidestream
Anammox
MBR
Inhibition
Metagenomics

ABSTRACT

Anaerobic ammonium oxidation (anammox) would be a feasible treatment method for thermal hydrolysis processed sidestream (THPS). Short-term study revealed that the 1/20 diluted THPS caused a 28% decrease of specific anammox activity. The MBR achieved a volumetric nitrogen loading rate of 3.64 kg/(m^3·d) with undiluted regular sidestream (RS) fed, while the reactor crashed with 70% diluted THPS as feed. The ratio of produced NO_3^--N to consumed NH_4^+-N also decreased compared with RS feeding. *Candidatus brocadia* was the major anammox bacteria species with the average abundance of 33.3% (synthetic wastewater), 6.42% (RS) and 2.51% (THPS). The abundances of metagenome bins for dissimilatory nitrate reduction to ammonium (DNRA) increased in the system with THPS compared with RS. The reason for the inhibition of anammox by THPS could be the high content of organic carbon in THPS, which caused the over-population of heterotrophic bacteria, i.e. DNRA bacteria, leading to anammox bacteria washout.

1. Introduction

Anaerobic ammonium oxidation (anammox), which is an autotrophic biological process, has drawn extensive attention as a novel and cost-effective alternative to remove nitrogen from wastewater. Anammox bacteria (AnAOB) directly convert ammonium to nitrogen gas using nitrite as electron acceptor under anaerobic condition, as shown in Eq. (1) (Strous et al., 1998).

$$NH_4^+ + 1.32NO_2^- + 0.066HCO_3^- + 0.13H^+ \rightarrow 0.066CH_2O_{0.5}N_{0.15} + 1.02N_2 + 2.03H_2O + 0.26NO_3^- \quad (1)$$

Due to its low energy consumption and negligible sludge production (van der Star et al., 2007), anammox has been successfully implemented to treat various types of ammonium-rich and low C/N wastewaters, such as landfill leachate, swine digester liquor, refinery wastewater and wastewater treatment plant (WWTP) sidestream (Ganigué et al., 2009; Milia et al., 2012; Yamamoto et al., 2008). The first full-scale anammox reactor was installed at the sludge treatment plant Sluisjesdijk, Rotterdam, NL in 2002 and such applications is becoming increasingly popular (Lackner et al., 2014).

Thermal hydrolysis process (THP) is a promising and energy-efficient pre-treatment process for anaerobic digestion (AD). It has proven to be successfully at improving AD efficiency by the combined actions of high pressure, heat and sudden de-pressurization, which can break down the organic matter, making it more available for bacteria to digest (Appels et al., 2010). Furthermore, THP lowers the bound water fraction in sludge, resulting in an increased cake solids concentration (Zhang et al., 2018). There are more than 20 full scale THP installations worldwide and the number is rapidly growing (Rus et al., 2017). The effluent of THP pre-treated AD is called THP pre-treated sidestream (THPS). Compared with regular sidestream (RS), THPS has a higher COD to nitrogen ratio, while still not enough for the conventional nitrification and denitrification processes.

Previous studies revealed THPS was inhibitory to the one-stage nitritation-anammox process (Zhang et al., 2016). Although it is believed that nitritation but not anammox process was inhibited by THPS, the effect of THPS on anammox process still needs to be elucidated. In previous studies, the anammox and partial nitrification processes were

* Corresponding author.
E-mail address: siqingxia@tongji.edu.cn (S. Xia).
[1] These two authors contribute equally.

https://doi.org/10.1016/j.biortech.2018.08.132
Received 30 June 2018; Received in revised form 29 August 2018; Accepted 30 August 2018
Available online 01 September 2018
0960-8524/

operated in one reactor treating up to 70% of THPS, therefore, it was difficult to distinguish inhibition kinetics specific to each process. Thus, it appears interesting to investigate the specific inhibition of THPS on a separate anammox process, which can provide not only a reference for the study of inhibition mechanisms but also a microbial evolution marker for tracking process performance with the presence of THPS. In addition, instead of operating a separate unit for partial nitritation, which could be intractable to control the nitrite to ammonium ratio in effluent, providing a relatively precise dosage of nitrite for anammox might be a practicable approach to treat sidestream (de Almeida Fernandes et al., 2018).

Various substrates and chemicals have been found to inhibit anammox process, including free ammonia (FA), free nitrous acid (FNA), organic matters, salts, heavy metals, phosphate and sulfide (Jin et al., 2012). Among all inhibitors, the effect of organic matters on anammox process is considered to be the key influence of THPS. Figdore et al. (2011) observed the elimination of inhibition by applying iron precipitants to remove soluble COD.

The mechanism of the effects of COD on anammox process could be associated with other heterotrophic pathway in the nitrogen cycle, such as dissimilatory nitrate reduction to ammonium (DNRA) and denitrification. The DNRA pathway is governed by chemoorganoheterotrophic bacteria, which are fast-growing microorganisms and can compete substrate with AnAOB. DNRA usually starts with nitrate reduction to nitrite, then ammonium, though it may also begin with nitrite (Lam and Kuypers, 2011). Being more efficient in energy yield compared with denitrification, DNRA pathway was demonstrated to be the dominant pathway of the nitrate/nitrite reduction in the tropical estuarine sediment (Dong et al., 2011). The coexistence of DNRA and anammox has been discovered in marine sediments, great lake, wetland and costal ecosystem (Jones et al., 2017). The cooperative action between DNRA and anammox can contribute to enhanced nitrogen removal (Castro-Barros et al., 2017). However, the occupation of DNRA pathway could out-compete anammox process by breaking ammonium to nitrite ratio for anammox feed, leading to AnAOB washout.

In previous studies, molecular biology approaches were used to reveal microbial community phylogeny, including denaturing gradient gel electrophoresis (DGGE) (Park et al., 2010a; Xiao et al., 2009), fluorescence in situ hybridization (FISH) (Hu et al., 2010; van der Star et al., 2007) and sequencing after cloning (Isanta et al., 2015; Wang et al., 2016). However, most of these methods are based on gene amplification which may cause technical biases (Aird et al., 2011) and provide limited information about the functional characteristics of cultures (Han et al., 2013). In this study, metagenomic analyses were conducted to reveal community-level functional profiling of the anammox system.

The objective of this study is to assess the inhibitory effects of THP on anammox process. The investigation is based on (a) short term study on specific anammox activity; (b) long term performance of anammox bioreactor treating RS and THPS; (c) taxonomic and functional compositions in anammox communities.

2. Materials and methods

2.1. Anammox enrichment

For better retention of anammox biomass, membrane biological reactors (MBR) was selected in present study. Anammox microorganisms was enriched in a 3-L submerged MBR reactor, inoculated with sludge from a deammonification pilot plant. A hydrophilic polyvinylidene fluoride (PVDF) hollow fiber membrane module was equipped with an effective filtration area of 0.02 m^2 and a nominal pore size of 0.22 μm (Li-tree Company, China). The reactor was fitted with a water jacket at a constant temperature (37.0 ± 0.5 °C) maintained by a heated recirculator (Model 1104, VWR, USA). Inert gas (95% Ar + 5% CO_2) was purged into the system to ensure anaerobic conditions and also provide inorganic carbon. The reactor was placed on a magnetic stirrer (C-MAG HS 7, IKA, Germany). Synthetic wastewater (SWW) was used to establish the anammox process with solid retention time (SRT) of 30–90 d and hydraulic retention time (HRT) of 1 d. The SWW contained (per 1 L deionized water): $(NH_4)_2SO_4$, 0.33–11.88 g; $NaNO_2$, 0.35–12.42 g; $KHCO_3$, 0–1.00 g; KH_2PO_4, 2.72 g; $MgCl_2{\cdot}6H_2O$, 24.76 g; $CaCl_2{\cdot}2H_2O$, 18.00 g; $FeCl_2{\cdot}4H_2O$, 17.89 g; and 1 ml of trace element solution II (Described by Van de Graaf et al. (1996)). Intermittent filtration was selected (10 min filtration and 2 min pause) using a permeation peristaltic pump. pH was controlled at 7.0 ± 0.1 by addition of bicarbonate buffer.

2.2. Shock loading assays

A set of shock loading assays were conducted on the 3-L reactor to study the effect of various feed on in situ activity of anammox microorganisms. Before each test, influent was cut off and $NaNO_2$ was added to lower the concentration of NH_4^+-N in the reactor to below 0.5 mg/L. Then RS and THPS were fed into the reactor with different dilution. Additional ammonium and nitrite were added into the diluted RS and THPS to reach the initial concentrations of 100 mg/L for both NH_4^+-N and NO_2^--N. SWW with same initial concentrations were also tested as a control group. For all the tests, pH were controlled at 6.8–7.0. After each shock load which lasted less than 1 h, the reactor was operated under normal conditions for 3 days to monitor long-term effects of the shock load. Each shock loading assay was repeated for three times.

The short-term responses of the anammox biomass to organic stress under the condition of a fixed initial substrate level were performed. Sodium acetate was used as the sole source of organic carbon. Four COD concentrations (50, 100, 200 and 500 mg/L) were adopted for test. The initial substrate level was set at 200 mg-TN/L with a ratio of NO_2^--N to NH_4^+-N of 1. For each experiment, the specific anammox activity (SAA = MSCR/VSS, where MSCR is the maximum substrate consumption rate) was recorded to investigate whether the performance of AnAOB was affected by COD addition. The RSAA (relative specific anammox activity) was calculated using the equation RSAA = SAA/SAA_{max}, where SAA_{max} is the maximum specific activity among assays.

2.3. Reactors operation

Enriched anammox biomass was transferred to two identical 1-L submerged MBR reactors treating regular sidestream (RS) and THP sidestream (THPS) respectively. Inert gas with higher CO_2 proportion (90% Ar + 10% CO_2) was selected due to higher alkalinity of the influent. Both RS and THPS were obtained from a municipal wastewater treatment plant (WWTP) located in Northern California, USA. The THPS was obtained after dewatering anaerobically digested sludge pretreated with THP (165 °C, 30 min), while the RS was obtained from sludge without THP. The sidestream was sealed in a plastic drum for storage at 4 °C after been transported from the WWTP. $NaNO_2$ was added to the influent with a ratio of NO_2^--N to NH_4^+-N of 1.1. SRT was set at 30 days.

2.4. Chemical analysis

The collected water samples were filtered through 0.45 μm membrane filters, stored at 4 °C, and analyzed within 1 day. The ammonium, nitrite and chemical oxygen demand were detected using commercial test kits (Hach, USA). The analysis was performed on a designated spectrophotometer (DR2400, Hach, USA). The nitrate was analyzed on an ion chromatograph (ICS-1100, Dionex, USA) with a Dionex IonPac AS23 IC Column (Dionex, USA). Dissolved Oxygen (DO) was detected with a portable dissolved oxygen meter (HQ40d, Hach, USA) equipped with a luminescent DO sensor. The alkalinity was determined by titrating the sample with sulfuric acid using a digital titrator (AL-DT, Hach, USA). Mixed liquor suspended solids (MLSS) and mixed liquor

volatile suspended solids (MLVSS) were measured according to US standard methods 2540D/E. Total organic carbon was determined by TOC-VCPH (SHIMADZU, Japan). The concentrations of carbohydrate and protein were measured by the phenol-sulfuric acid method and the Branford method, respectively. The molecular weight (MW) distributions were studied using a gel filtration chromatography analyzer (LC-10ADVP, Shimadzu, Japan). Three-dimensional EEM fluorescence spectroscopy was determined by a luminescence spectrometry (F-4500FL, Hitachi, Japan) and processed by the software Origin 8.0 (OriginLab, USA). EEM spectra were collected with corresponding scanning emission spectra from 300 nm to 550 nm at 5 nm increments by varying the excitation wavelengths from 240 nm to 450 nm at 5 nm sampling intervals. The excitation and emission slits were maintained at 10 nm and the scanning speed was 1200 nm/min.

2.5. DNA extraction

Three replicates of 2-mL samples were collected from each reactor every week. DNA extraction was performed on biomass pellet after centrifuge at 13,000*g* for 10 min at 4 °C using PowerSoil DNA Isolation Kit (MO-BIO, USA) following manufacturer's instruction. DNA concentration and purity were determined by NanoDrop micro-spectrophotometry (ND-1000, Thermo Fisher, USA).

2.6. 16S rRNA sequencing

16S rRNA genes were amplified from the DNA extracts in triplicate using primers 515FB (GTGYCAGCMGCCGCGGTAA) and 806RB (GGACTACNVGGGTWTCTAAT), which was modified from the 515F-806R primer pair (Caporaso et al., 2011) and targeted the V4 region of bacterial 16S rRNA gene (Parada et al., 2016).

The PCR amplification was conducted in a 50-μl reaction system using Platinum Hot Start PCR Master Mix (Thermo Fisher, USA). Reaction conditions were 94 °C for 3 min, 94 °C for 45 s, 50 °C for 60 s, 72 °C for 90 s, repeat steps 2–4 30 times and 72 °C for 10 min. Libraries were prepared for paired 300-bp in MiSeq V3 platform (Illumina, USA) at The California Institute for Quantitative Biosciences (QB3) at UC Berkeley and run in 1 lane.

The reads which contained one or more ambiguous bases ('N') were removed for quality control. The filtered 16S rRNA gene sequences were further processed following the Mothur MiSeq SOP pipeline (Kozich et al., 2013) (http://www.mothur.org/wiki/MiSeq_SOP) to demultiplex and conduct further quality control. Then QIIME (v1.8.0) was applied for open-reference operational taxonomic unit (OTU) picking at cutoff of 98.7% (Yarza et al., 2014) and Uclust (Edgar, 2010) was applied to assign OTU at 80% confidence level against Silva database (release 123) (Quast et al., 2012).

2.7. Metagenomic analysis

Sequence libraries of ~350-bp DNA fragments were prepared and then sequenced by Illumina HiSeq 4000 (paired-end 150 bp). About 10 Gb (giga base pairs) of sequencing data were generated for one sample. 'Omics' raw reads were removed when the ambiguous nucleotides were more than 10% or more than 20% nucleotides had the quality scores of less than 20.

A modified bi-dimension binning process was applied to recover the genomes of dominant species from metagenomic datasets (Albertsen et al., 2013). Contigs grouped by bi-dimension coverage, which were further clustered by tetranucleotide frequency and paired-end tracking, were extracted from the contig pool as binned genomes. The trimmed paired-end reads were assembled by CLCbio de novo assembly algorithm, using a k-mer of 63 and a minimum contig length of 1 kbp. Reads were then individually mapped to scaffolds using CLCbio with a minimum similarity of 95% over 100% of the read length. A genome evaluation software, checkM, was used to evaluate the genome completeness using marker genes (Parks et al., 2015).

Contigs were submitted to MetaProdigal (Hyatt et al., 2012) for open reading frame (ORF) calling. ORFs were further BLASTx against KEGG and NCBI-nr database with an e-value of 1e−5 for functional annotation. Integration and visualization of KEGG blast results were performed by Pathview (Luo and Brouwer, 2013). Simultaneously, novel sequences functional prediction was performed by Pfam (Finn et al., 2015). Annotation outputs were further manually checked.

3. Results and discussion

3.1. Anammox enrichment

The anammox enrichment period lasted 1 year. Anammox process was successfully established in the MBR with a maximum influent TN concentration of 5292 mg/L. The volumetric nitrogen loading rate reached 4.12 kg/(m^3·d), and more than 90% nitrogen removal was achieved. The color of the biomass changed from greyish black to dark red, which was accompanied by an increase in cytochrome content (Van de Graaf et al., 1996). The concentration of nitrite in the reactor remained below 20 mg/L. The average ratio of consumed NO_2^--N/consumed NH_4^+-N and produced NO_3^--N/consumed NH_4^+-N was 1.18 and 0.16 respectively, which were lower than the theoretical values of 1.32 and 0.26. This indicated the formation of ammonium or reduction of nitrate, which was possibly done by dissimilatory nitrate reduction or denitrification.

3.2. Characteristics of sidestream

The characteristics of RS and THPS are summarized in Table 1. Compared with RS, THPS contained much higher concentrations of NH_4^+-N and COD. The average molecular weight of THPS was only 59% of which of RS. EEM analysis was carried out identify the dissolved organic matters properties of RS and THPS. The results are illustrated in Fig. 1. It was evident that two peaks for RS can be clearly identified from the EEM fluorescence spectra compared to THPS. Peak B was observed at the excitation/emission (Ex/Em) of 320–360/420–460 nm, which had been reported as humic acid-like peak. Peak C located at the Ex/Em of 245–255/450–470 nm was related to fulvic acid-like substances (Chen et al., 2003). The results suggested THP pretreatment increased the biological degradation of sludge, resulting in a higher content of easy biodegradable organic matters.

3.3. Short term study

Four different inhibition models, including non-competitive inhibition kinetic model (Eq. (2), Carrera et al. (2003)), extended non-competitive inhibition kinetic model (Eq. (3)) and Luong inhibition kinetic model (Eq. (4), Luong (1985)) were applied to represent the inhibitory characteristics of COD inhibition on anammox.

Table 1
Wastewater quality of RS and THPS.

(mg/L)	RS	THPS
TOC	229.4 ± 32.9	851.7 ± 95.3
NH_4^+-N	1420 ± 130	2190 ± 280
NO_2^--N	0.9 ± 0.1	0.1 ± 0.1
NO_3^--N	0.3 ± 0.1	0.4 ± 0.2
TP	82 ± 7	88 ± 9
COD	841 ± 186	3290 ± 640
BOD_5	162.5 ± 78.3	834.6 ± 162.5
Alkalinity ($CaCO_3$)	3260 ± 670	5000 ± 1280
Protein	241.9 ± 16.9	657.5 ± 47.1
Polysaccharide	8.7 ± 1.2	191.3 ± 16.3
Average MW	15000 Da	8900 Da

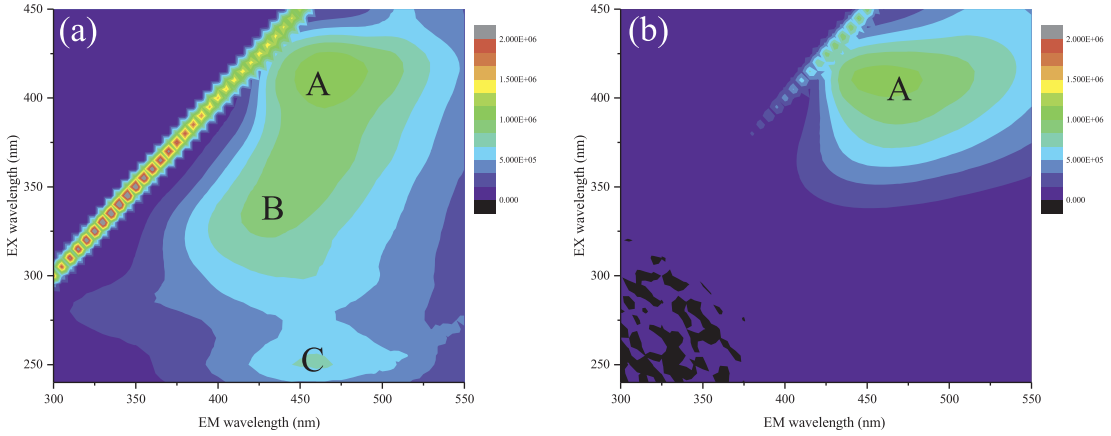

Fig. 1. EEM fluorescence spectra of RS (a) and THPS (b).

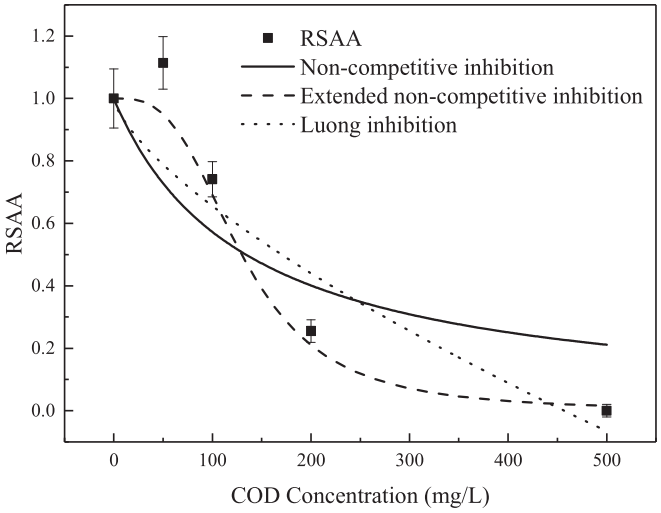

Fig. 2. RSAA (relative specific anammox activity) at different COD concentrations.

$$RSAA = \frac{K_I}{I + K_I} \quad (2)$$

$$RSAA = \frac{K_I}{I^m + K_I} \quad (3)$$

$$RSAA = 1-(\frac{I}{K_{IL}})^n \quad (4)$$

Table 2
Number of sequence and estimated diversity indices.

Sample	Sequence	Shannon	Simpson	Ace	Chao	Coverage
SWW_1	440,883	1.935351	0.283004	294.1963	286.2069	0.999689
SWW_2	554,262	1.984516	0.281352	407.8227	418.3438	0.999593
RS_1	372,980	3.884917	0.068093	1284.34	1301.162	0.998044
RS_2	439,706	4.002663	0.056955	1211.569	1274.124	0.998398
THPS_1	460,097	3.451653	0.078091	863.9655	802.3684	0.998965
THPS_2	519,935	3.557315	0.068544	973.1314	872.7143	0.9987

where, K_I is the non-competitive inhibition constant, K_{IL} is the Luong inhibition constant, m is the extended constant for non-competitive inhibition, n is the Luong constant, I is the inhibitor concentration.

The RSAA at different COD concentrations and the fitting results are shown in Fig. 2. The anammox biomass did not show any stress under the shock loading of 50 mg/L COD. In fact, in the case of experiments with low COD concentrations, an increase of anammox performance was observed. This was in accord with previous studies (Dapena-Mora et al., 2007; Van de Graaf et al., 1996), which could be due to the capacity of the AnAOB to carry out organic oxidation simultaneously with anaerobic ammonium oxidation (Güven et al., 2005). COD concentrations of 100 mg/L and 200 mg/L resulted in 26 and 74% inhibition percentage. The anammox activity completely lost at 500 mg/L COD, which was similar with the previous finding that 487.5 mg/L of COD inhibited anammox metabolism (Leal et al., 2016). The short-term effects of organic matter on anammox activity could be described by extended non-competitive inhibition kinetic model. The quantitative relationship between the inhibition response and the concentration of COD could be expressed by the following Equation.

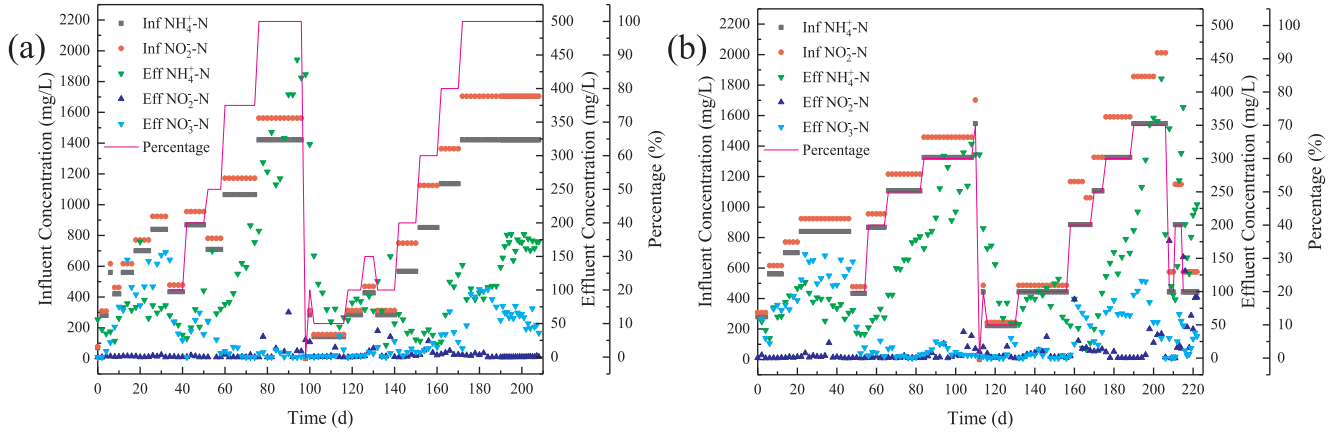

Fig. 3. Performance of MBR fed with RS (a) and THPS (b).

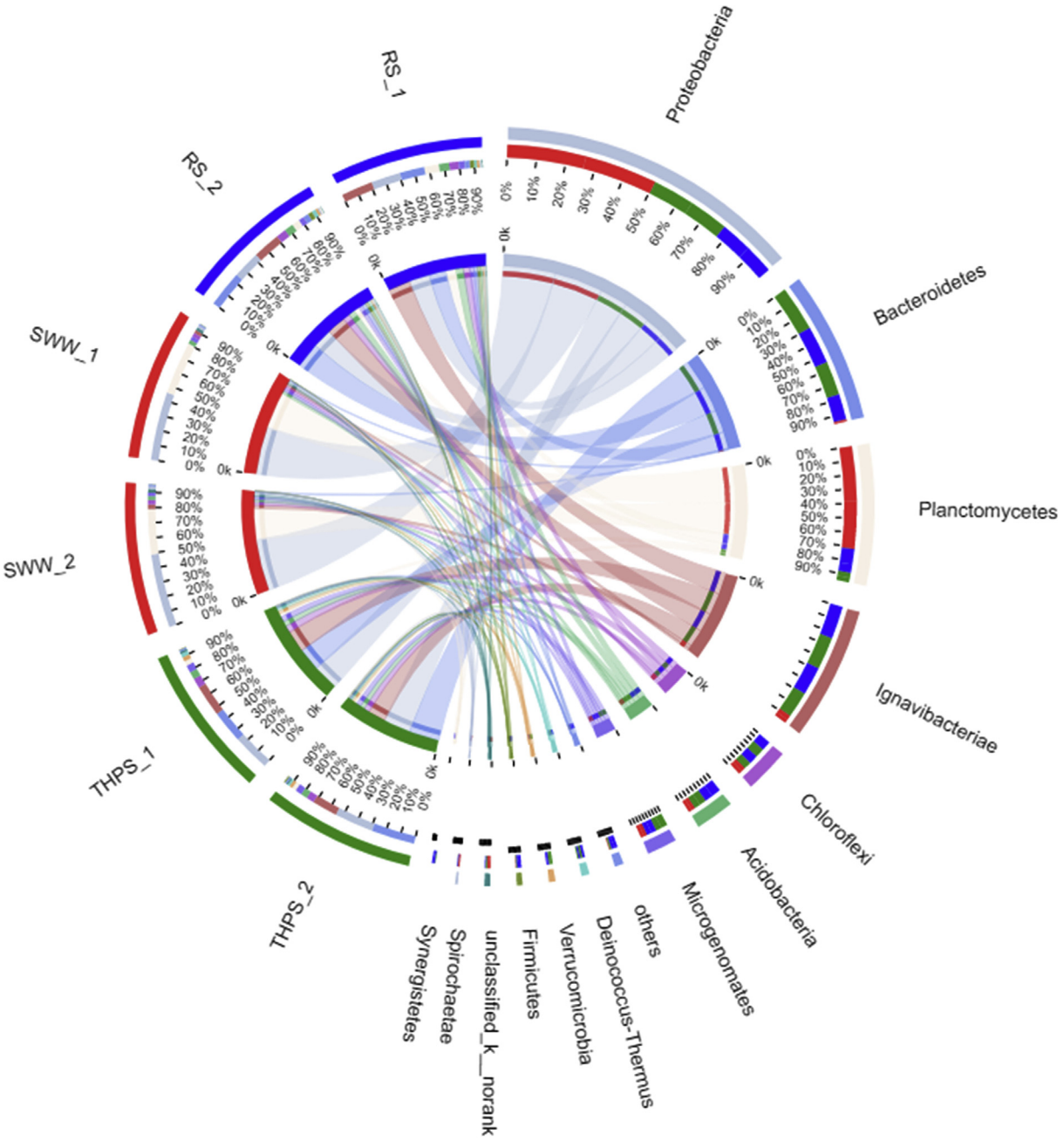

Fig. 4. Relative abundances of detected phyla in the six samples. The data were visualized via Circos software (Krzywinski et al., 2009).

$$\mathrm{RSAA} = \frac{2.95156 \times 10^6}{I^{3.06099} + 2.95156 \times 10^6} \quad (5)$$

To explore the effect of sidestream on the activity of AnAOB, instantaneous shock load of RS and THPS was applied. To eliminate the substrate inhibition, three levels of sidestream input (1/20 RS, 1/14 RS and 1/20 THPS) were chosen. $(NH_4)_2SO_4$ was added to 1/20 RS, so that the initial NH_4^+-N concentration for all input was 100 mg/L. $NaNO_2$ was added with a ratio of NH_4^+-N to NO_2^--N of 1. The SAA with the inputs of SWW, 1/20 RS, 1/14 RS and 1/20 THPS were 53.54, 68.68, 52.09 and 38.48 mg-N·h^{-1}·g-VSS^{-1}, respectively. 1/14 RS did not have a notable effect on anammox activity, and an increase of SAA was observed under 1/20 RS, which could be attributed to low COD concentration. 1/20 THPS with high COD concentration caused a decrease of 28% of SAA. The findings implied that the COD in THPS was the inhibitor on AnAOB activity. With the COD/N ratio increased from 0 (SWW), 0.42 (1/20 RS), 0.60 (1/14 RS) to 1.65 (1/20 THPS), the SAA decreased by 28%. Previous study revealed that anammox process was inhibited by 20% with COD/N ratio of 3.1 (Ni et al., 2012). On the other hand, it was also reported that a COD/N ratio of 5 didn't affect anammox performance (Leal et al., 2016). The different results might be due to the different testing conditions and the differences between batch tests and continuous flow reactors.

3.4. Long-term study

Two identical 1-L MBR reactors were inoculated with the same cultivated sludge and operated in parallel. The reactors were fed the diluted RS and THPS respectively. The percentage was increased periodically when the reactors reached stable stages. pH was controlled at 7.2 ± 0.2 by adding hydrochloric acid.

The performance of MBRs fed with RS and THPS is represented in Fig. 3(a), (b) respectively. As shown in Fig. 3(a), the diluted RS was

Fig. 5. Sequences assignment results at the genus level.

used beginning from 34 d at an influent concentration of NH_4^+-N that was diluted to 434 mg/L. The load was increased in steps to undiluted sidestream. The increase of load led to a moderate increase of effluent NO_2^--N concentration, which was gradually reduced when the system was operated for some time after the load increased. The achieved volumetric nitrogen loading rate was 3.64 kg/(m^3·d) and the removal efficiency of TN was above 90% with 100% RS influent feeding. The results suggested that the microorganisms gradually adapted to the RS and the anammox process was successful for the undiluted RS. In addition, NO_3^--N did not massively accumulate, and the ratio of produced NO_3^--N to consumed NH_4^+-N was in the range of 0.013–0.076 that was much lower than the system with SWW. This indicated the increased presence of DNRA or denitrification in the system fed with RS.

In the meanwhile, the reactor fed with diluted THPS experienced the similar operational phases. However, inhibition was observed during 70% THPS feeding. The NH_4^+-N and NO_2^--N concentration in the effluent increased rapidly and synchronously, which marked the

Table 3
Summary of bin-genome reconstruction from metagenomes.

ID	Completeness	Contamination	Genome size	Longest contig
102-Proteobacteria	98.37931034	5.205938697	3,011,495	102,800
106-Proteobacteria	98.25949367	2.215189873	3,692,182	341,356
113-Planctomycetes	96.59090909	0	3,376,503	256,355
115-Planctomycetes	98.9010989	1.648351648	3,018,561	268,974
117-Proteobacteria	99.33127572	3.209876543	3,459,507	117,234
119-Deinococcus-Thermus	90.04237288	1.200564972	2,885,193	188,468
124-Kryptonia	43.10344828	0	1,453,824	177,305
125-Ignavibacteriae	96.64804469	0.391061453	3,552,762	165,826
127-Bacteroidetes	82.5136612	0.364298725	2,054,384	243,136

washing-out of biomass. The maximum volumetric nitrogen loading rate was 3.40 kg/(m^3·d), lower than that of RS. Also, the ratio of produced NO_3^--N to consumed NH_4^+-N was around 0.01, lower than which of the system with RS feeding. The results stated that the inhibition was not caused by the substrate level, while it could be attributed to the high content of organic carbon in THPS, which led to the growth of heterotrophic bacteria. The long-term study illustrated that long-term acclimation cannot eliminate the inhibition of anammox by THP.

3.5. Microbial structures analysis

Six DNA samples were collected from the reactors treating SWW, RS and THPS. For each reactor, biomass samples were collected at two time points in the late phase of the experiments. A total of 2,787,863 effective sequences were obtained from 6 samples, which were clustered into 1392 OTUs at a distance of 0.03. The bacteria coverage described as the Good's value was between 99.80% and 99.97%, so the sequencing depth was sufficient to describe patterns (Table 2). Shannon, Ace and Simpson diversity indexes were applied to analyze the community richness and diversity (Table 2). These results demonstrated that the RS and THPS samples had more community richness and diversity compared with SWW samples, which was because of the complex composition of sidestream. Fig. 4 illustrates the phylum level distributions of bacterial sequences. The structures of microbial communities were significantly different across samples, and there was an obvious distinction between SWW and real wastewater communities. The phyla of *Proteobacteria* (47.4%–51.3% of the identified 16S rRNA gene fragments) and *Planctomycetes* (31.5%–36.8%) were dominant in SWW samples, while *Proteobacteria* (19.2%–27.2%), *Bacteroidetes* (16.7%–30.1%) and *Ignavibacteriae* (17.6%–21.9%) were dominant in both RS and THPS samples. The average relative abundance of *Planctomycetes* in RS and THPS samples was 7.95% and 3.20%, respectively. Previous studies reported that uncultured members of the phyla *Proteobacteria*, *Bacteroidetes*, *Chlorobi* and *Chloroflexi* are omnipresent in anammox bioreactors besides *Planctomycetes* (Park et al., 2010b; Speth et al., 2016). *Ignavibacteriae*, affiliated with *Chloroflexi*, are also frequently found in anammox reactors treating high organic content wastewater (Leal et al., 2016).

A total of 582 microbial genera were detected in six samples. The relative abundances of different genera and the phylogenetic tree are presented in Fig. 5. The *Candidatus Brocadia* was the major anammox bacteria species in the system with the abundance of 35.9% (SWW_1), 30.7% (SWW_2), 8.30% (RS_1), 4.35% (RS_2), 2.36% (THPS_1) and 1.94% (THPS_1), followed by SM1A02 (< 1% in all samples). It was reported that *Candidatus Brocadia* was more competitive than other AnAOB in the presence of acetate (Kartal et al., 2007; Winkler et al., 2012), and it was also found that the dominant *Candidatus Brocadia* did not contribute much to acetate oxidation (Jenni et al., 2014). The reactor also fostered a fairly high level of denitrifying bacteria, and the most predominant denitrifying bacteria were classified into the genus of *Denitratisoma*. The abundances of *Denitratisoma* in SWW_1, SWW_2, RS_1, RS_2, THPS_1 and THPS_2 were 39.2%, 43.1%, 0.591%, 0.569%, 3.02% and 2.73%. The observation was coincident with the study of Bae et al. (2010), which reported that the most predominant bacteria in the anammox UASB reactor were affiliated with *Denitratisoma oestradiolicum* (40%), and *Denitratisoma oestradiolicum* was reported to be able to reduce nitrate to a mixture of nitrogen gas and dinitrogen monoxide via nitrite as intermediate. Notably, the bacteria communities was diverse in the RS reactor with only 4.35%–8.30% of *Candidatus brocadia*, though high efficiency of NH_4^+-N and NO_2^--N removal was obtained. Furthermore, there was a sharp drop of denitrifier abundance in community compared to SWW samples as well. It can be inferred that due to the lower growth rate of AnAOB (yield coefficient of 0.066 ± 0.01 g-VSS/g-NH_4^+-N) (Strous et al., 1998), other heterotrophic bacteria, i.e. DNRA bacteria, multiplied with the application of sidestream influent.

3.6. Metagenomic analysis

A total of 392 884 712 reads from the samples metagenomes were filtered out after quality control and dynamic trimming, with an average length of 150 bp. Using de novo assembly, 451 Mbp of contigs with an average length of 4.4 kbp were obtained. The coverages of the assembled contigs for the samples metagenomes were between 92.4% and 96%, which indicate a reliable accuracy of the de novo assembly. In total, 127 metagenome bins were retrieved, and 9 metagenome bins with relatively high coverage and long contig length were subjected to further analysis (Table 3). The bins were functionally annotated using the Kyoto Encyclopedia of Genes and Genomes (KEGG).

Among 9 metagenome bins, 115-Planctomycetes was discovered to have a complete anammox pathway, which contained the key anammox enzymes, including hydrazine synthase (Hzs) and hydrazine dehydrogenase (Hhd). It is notable that 115-Planctomycetes also contained a DNRA pathway, which indicated anammox bacteria can be rather versatile in their metabolisms (Lam and Kuypers, 2011). However, due to the limited metabolic pathway of organic carbon, DNRA could just be an alternative pathway for AnAOB. In addition, there was a complete B12 synthetic pathway in 115-Planctomycetes, which was not found in other abundant metagenome bins. It indicated that AnAOB

Table 4
Abundances of metagenome bins in the six samples.

ID	SWW_1	SWW_2	RS_1	RS_2	THPS_1	THPS_2
102-Proteobacteria	0.074%	0.069%	0.587%	1.122%	0.638%	0.794%
106-Proteobacteria	2.482%	2.439%	0.361%	0.590%	0.522%	0.441%
113-Planctomycetes	0.497%	0.399%	0.758%	0.357%	0.340%	0.412%
115-Planctomycetes	35.446%	30.550%	5.227%	6.849%	1.183%	0.996%
117-Proteobacteria	21.761%	22.483%	2.329%	2.845%	7.830%	7.898%
119-Deinococcus-Thermus	0.005%	0.006%	1.303%	1.774%	1.303%	0.846%
124-Kryptonia	1.490%	1.789%	14.832%	12.360%	10.931%	9.091%
125-Ignavibacteriae	18.512%	18.778%	16.907%	17.823%	15.633%	15.659%
127-Bacteroidetes	6.046%	8.027%	41.085%	40.999%	53.349%	53.173%

could be the source of B12 for other bacteria. The DNRA pathway was also discovered in many metagenome bins, including 106-Proteobacteria, 124-Kryptonia and 127-Bacteroidetes. 117-Proteobacteria and 119-Deinococcus-Thermus are related to denitrification. 125-Ignavibacteriacea is related to degradation of starch, sugars and peptides and thus involved in COD removal. 124-Kryptonia contains key metabolic enzymes for Embden-Meyerhof glycolysis and the pentose phosphate pathway. The abundances of metagenomes for the six samples are presented in Table 4. As shown, the percentage of 115-Planctomycetes in SWW_1, SWW_2, RS_1, RS_2, THPS_1 and THPS_2 were 35.446%, 30.550%, 5.227%, 6.849%, 1.183% and 0.996%, which was in line with the 16S results. The average abundances of metagenomes associated with DNRA in SWW, RS and THPS samples were 11.137%, 54.614% and 63.753%, respectively. The results implied that DNRA was one of the major pathway in the system. The DNRA bacteria more populated in the system with THPS fed compared with RS.

Both DNRA and denitrification processes can be coupled with anammox for its NH_4^+ requirements. It was reported that DNRA can generate more energy from unit nitrate reduced than denitrifier, and therefore, have certain competitive advantages over denitrifiers in nitrate-limiting and organic-rich settings (Dong et al., 2011; Lam and Kuypers, 2011). The co-existence of DNRA and anammox in the reactor illustrated the synergetic association for nitrogen removal. However, the over population of DNRA bacteria could out-compete AnAOB by breaking ammonium to nitrite ratio for anammox feed, leading to the washing-out of AnAOB, which may elucidate the crash of the THPS reactor.

4. Conclusions

The THP pre-treated sidestream had inhibitory effects on the activity of anammox bacteria, and long-term acclimation cannot eliminate the inhibition, while anammox process worked well with regular sidestream under the help of dissimilatory nitrate reduction to ammonium. The reason for the inhibition could be the high content of organic carbon in the THP pre-treated sidestream, which caused the over-population of heterotrophic bacteria, leading to the washout of anammox bacteria. This study would assist the future design of anammox processes for THP sidestream treatment.

Acknowledgements

The authors sincerely thank the support of National Key Research and Development Program of China (2017YFC0403400) and Thousand Talents Program. In-kind support of the San Francisco Public Utilities Commission Wastewater Enterprise and its staff is also gratefully acknowledged.

References

Aird, D., Ross, M.G., Chen, W.-S., Danielsson, M., Fennell, T., Russ, C., Jaffe, D.B., Nusbaum, C., Gnirke, A., 2011. Analyzing and minimizing PCR amplification bias in Illumina sequencing libraries. Genome Biol. 12 (2), R18.

Albertsen, M., Hugenholtz, P., Skarshewski, A., Nielsen, K.L., Tyson, G.W., Nielsen, P.H., 2013. Genome sequences of rare, uncultured bacteria obtained by differential coverage binning of multiple metagenomes. Nat. Biotechnol. 31 (6), 533-+.

Appels, L., Degrève, J., Van der Bruggen, B., Van Impe, J., Dewil, R., 2010. Influence of low temperature thermal pre-treatment on sludge solubilisation, heavy metal release and anaerobic digestion. Bioresour. Technol. 101 (15), 5743–5748.

Bae, H., Chung, Y.-C., Jung, J.-Y., 2010. Microbial community structure and occurrence of diverse autotrophic ammonium oxidizing microorganisms in the anammox process. Water Sci. Technol. 61 (11), 2723–2732.

Caporaso, J.G., Lauber, C.L., Walters, W.A., Berg-Lyons, D., Lozupone, C.A., Turnbaugh, P.J., Fierer, N., Knight, R., 2011. Global patterns of 16S rRNA diversity at a depth of millions of sequences per sample. Proc. Natl. Acad. Sci. 108 (Suppl. 1), 4516–4522.

Carrera, J., Torrijos, M., Baeza, J.A., Lafuente, J., Vicent, T., 2003. Inhibition of nitrification by fluoride in high-strength ammonium wastewater in activated sludge. Process Biochem. 39 (1), 73–79.

Castro-Barros, C.M., Jia, M., van Loosdrecht, M.C.M., Volcke, E.I.P., Winkler, M.K.H., 2017. Evaluating the potential for dissimilatory nitrate reduction by anammox bacteria for municipal wastewater treatment. Bioresour. Technol. 233, 363–372.

Chen, W., Westerhoff, P., Leenheer, J.A., Booksh, K., 2003. Fluorescence excitation-emission matrix regional integration to quantify spectra for dissolved organic matter. Environ. Sci. Technol. 37 (24), 5701–5710.

Dapena-Mora, A., Fernandez, I., Campos, J., Mosquera-Corral, A., Mendez, R., Jetten, M., 2007. Evaluation of activity and inhibition effects on anammox process by batch tests based on the nitrogen gas production. Enzyme Microb. Technol. 40 (4), 859–865.

de Almeida Fernandes, L., Pereira, A.D., Leal, C.D., Davenport, R., Werner, D., Mota Filho, C.R., Bressani-Ribeiro, T., de Lemos Chernicharo, C.A., de Araújo, J.C., 2018. Effect of temperature on microbial diversity and nitrogen removal performance of an anammox reactor treating anaerobically pretreated municipal wastewater. Bioresour. Technol. 258, 208–219.

Dong, L.F., Sobey, M.N., Smith, C.J., Rusmana, I., Phillips, W., Stott, A., Osborn, A.M., Nedwell, D.B., 2011. Dissimilatory reduction of nitrate to ammonium, not denitrification or anammox, dominates benthic nitrate reduction in tropical estuaries. Limnol. Oceanogr. 56 (1), 279–291.

Edgar, R.C., 2010. Search and clustering orders of magnitude faster than BLAST. Bioinformatics 26 (19), 2460–2461.

Figdore, B., Wett, B., Hell, M., Murthy, S., 2011. Deammonification of dewatering sidestream from thermal hydrolysis-mesophilic anaerobic digestion process. Proc. Water Environ. Feder. 2011 (1), 1037–1052.

Finn, R.D., Coggill, P., Eberhardt, R.Y., Eddy, S.R., Mistry, J., Mitchell, A.L., Potter, S.C., Punta, M., Qureshi, M., Sangrador-Vegas, A., 2015. The Pfam protein families database: towards a more sustainable future. Nucl. Acids Res. 44 (D1), D279–D285.

Ganigué, R., Gabarró, J., Sànchez-Melsió, A., Ruscalleda, M., López, H., Vila, X., Colprim, J., Balaguer, M.D., 2009. Long-term operation of a partial nitritation pilot plant treating leachate with extremely high ammonium concentration prior to an anammox process. Bioresour. Technol. 100 (23), 5624–5632.

Güven, D., Dapena, A., Kartal, B., Schmid, M.C., Maas, B., van de Pas-Schoonen, K., Sozen, S., Mendez, R., den Camp, H.J.O., Jetten, M.S., 2005. Propionate oxidation by and methanol inhibition of anaerobic ammonium-oxidizing bacteria. Appl. Environ. Microbiol. 71 (2), 1066–1071.

Han, P., Huang, Y.-T., Lin, J.-G., Gu, J.-D., 2013. A comparison of two 16S rRNA gene-based PCR primer sets in unraveling anammox bacteria from different environmental samples. Appl. Microbiol. Biotechnol. 97 (24), 10521–10529.

Hu, B.L., Zheng, P., Tang, C.J., Chen, J.W., van der Biezen, E., Zhang, L., Ni, B.J., Jetten, M.S., Yan, J., Yu, H.Q., Kartal, B., 2010. Identification and quantification of anammox bacteria in eight nitrogen removal reactors. Water Res. 44 (17), 5014–5020.

Hyatt, D., LoCascio, P.F., Hauser, L.J., Uberbacher, E.C., 2012. Gene and translation initiation site prediction in metagenomic sequences. Bioinformatics 28 (17), 2223–2230.

Isanta, E., Bezerra, T., Fernández, I., Suárez-Ojeda, M.E., Pérez, J., Carrera, J., 2015. Microbial community shifts on an anammox reactor after a temperature shock using 454-pyrosequencing analysis. Bioresour. Technol. 181, 207–213.

Jenni, S., Vlaeminck, S.E., Morgenroth, E., Udert, K.M., 2014. Successful application of nitritation/anammox to wastewater with elevated organic carbon to ammonia ratios. Water Res. 49, 316–326.

Jin, R.-C., Yang, G.-F., Yu, J.-J., Zheng, P., 2012. The inhibition of the anammox process: a review. Chem. Eng. J. 197, 67–79.

Jones, Z.L., Jasper, J.T., Sedlak, D.L., Sharp, J.O., 2017. Sulfide-induced dissimilatory nitrate reduction to ammonium supports anaerobic ammonium oxidation (anammox) in an open-water unit process wetland. Appl. Environ. Microbiol. 83 (15).

Kartal, B., Rattray, J., van Niftrik, L.A., van de Vossenberg, J., Schmid, M.C., Webb, R.I., Schouten, S., Fuerst, J.A., Damste, J.S.S., Jetten, M.S.M., Strous, M., 2007. Candidatus "Anammoxoglobus propionicus" a new propionate oxidizing species of anaerobic ammonium oxidizing bacteria. Syst. Appl. Microbiol. 30 (1), 39–49.

Kozich, J.J., Westcott, S.L., Baxter, N.T., Highlander, S.K., Schloss, P.D., 2013. Development of a dual-index sequencing strategy and curation pipeline for analyzing amplicon sequence data on the MiSeq Illumina sequencing platform. Appl. Environ. Microbiol. 79 (17), 5112–5120.

Krzywinski, M., Schein, J., Birol, I., Connors, J., Gascoyne, R., Horsman, D., Jones, S.J., Marra, M.A., 2009. Circos: an information aesthetic for comparative genomics. Genome Res. 19 (9), 1639–1645.

Lackner, S., Gilbert, E.M., Vlaeminck, S.E., Joss, A., Horn, H., van Loosdrecht, M.C.M., 2014. Full-scale partial nitritation/anammox experiences – an application survey. Water Res. 55, 292–303.

Lam, P., Kuypers, M.M., 2011. Microbial nitrogen cycling processes in oxygen minimum zones. Annu. Rev. Mar. Sci. 3 (1), 317–345.

Leal, C.D., Pereira, A.D., Nunes, F.T., Ferreira, L.O., Coelho, A.C.C., Bicalho, S.K., Mac Conell, E.F.A., Ribeiro, T.B., de Lemos Chernicharo, C.A., de Araújo, J.C., 2016. Anammox for nitrogen removal from anaerobically pre-treated municipal wastewater: effect of COD/N ratios on process performance and bacterial community structure. Bioresour. Technol. 211, 257–266.

Luo, W., Brouwer, C., 2013. Pathview: an R/bioconductor package for pathway-based data integration and visualization. Bioinformatics 29 (14), 1830–1831.

Luong, J., 1985. Kinetics of ethanol inhibition in alcohol fermentation. Biotechnology and bioengineering 27 (3), 280–285.

Milia, S., Cappai, G., Perra, M., Carucci, A., 2012. Biological treatment of nitrogen-rich refinery wastewater by partial nitritation (SHARON) process. Environ. Technol. 33 (13), 1477–1483.

Ni, S.-Q., Ni, J.-Y., Hu, D.-L., Sung, S., 2012. Effect of organic matter on the performance of granular anammox process. Bioresour. Technol. 110, 701–705.

Parada, A.E., Needham, D.M., Fuhrman, J.A., 2016. Every base matters: assessing small subunit rRNA primers for marine microbiomes with mock communities, time series and global field samples. Environ. Microbiol. 18 (5), 1403–1414.

Park, H., Rosenthal, A., Jezek, R., Ramalingam, K., Fillos, J., Chandran, K., 2010a. Impact

of inocula and growth mode on the molecular microbial ecology of anaerobic ammonia oxidation (anammox) bioreactor communities. Water Res. 44 (17), 5005–5013.
Park, H., Rosenthal, A., Ramalingam, K., Fillos, J., Chandran, K., 2010b. Linking community profiles, gene expression and N-removal in anammox bioreactors treating municipal anaerobic digestion reject water. Environ. Sci. Technol. 44 (16), 6110–6116.
Parks, D.H., Imelfort, M., Skennerton, C.T., Hugenholtz, P., Tyson, G.W., 2015. CheckM: assessing the quality of microbial genomes recovered from isolates, single cells, and metagenomes. Genome Res. 25 (7), 1043–1055.
Quast, C., Pruesse, E., Yilmaz, P., Gerken, J., Schweer, T., Yarza, P., Peplies, J., Glöckner, F.O., 2012. The SILVA ribosomal RNA gene database project: improved data processing and web-based tools. Nucl. Acids Res. 41 (D1), D590–D596.
Rus, E., Perrault, A., Mills, N., Shana, A., Molokwu, O., Nilsen, P., 2017. Optimizing THP—the intermediate thermal hydrolysis process. Proc. Water Environ. Feder. 2017 (1), 42–49.
Speth, D.R., Guerrero-Cruz, S., Dutilh, B.E., Jetten, M.S., 2016. Genome-based microbial ecology of anammox granules in a full-scale wastewater treatment system. Nat. Commun. 7, 11172.
Strous, M., Heijnen, J.J., Kuenen, J.G., Jetten, M.S.M., 1998. The sequencing batch reactor as a powerful tool for the study of slowly growing anaerobic ammonium-oxidizing microorganisms. Appl. Microbiol. Biotechnol. 50 (5), 589–596.
Van de Graaf, A.A., de Bruijn, P., Robertson, L.A., Jetten, M.S., Kuenen, J.G., 1996. Autotrophic growth of anaerobic ammonium-oxidizing micro-organisms in a fluidized bed reactor. Microbiology 142 (8), 2187–2196.
van der Star, W.R.L., Abma, W.R., Blommers, D., Mulder, J.-W., Tokutomi, T., Strous, M., Picioreanu, C., van Loosdrecht, M.C.M., 2007. Startup of reactors for anoxic ammonium oxidation: Experiences from the first full-scale anammox reactor in Rotterdam. Water Res. 41 (18), 4149–4163.
Wang, B., Peng, Y., Guo, Y., Zhao, M., Wang, S., 2016. Illumina MiSeq sequencing reveals the key microorganisms involved in partial nitritation followed by simultaneous sludge fermentation, denitrification and anammox process. Bioresour. Technol. 207, 118–125.
Winkler, M.-K., Kleerebezem, R., Van Loosdrecht, M., 2012. Integration of anammox into the aerobic granular sludge process for main stream wastewater treatment at ambient temperatures. Water Res. 46 (1), 136–144.
Xiao, Y., Zeng, G., Yang, Z., Liu, Y.S., Ma, Y., Yang, L., Wang, R., Xu, Z.Y., 2009. Coexistence of nitrifiers, denitrifiers and Anammox bacteria in a sequencing batch biofilm reactor as revealed by PCR-DGGE. J. Appl. Microbiol. 106 (2), 496–505.
Yamamoto, T., Takaki, K., Koyama, T., Furukawa, K., 2008. Long-term stability of partial nitritation of swine wastewater digester liquor and its subsequent treatment by anammox. Bioresour. Technol. 99 (14), 6419–6425.
Yarza, P., Yilmaz, P., Pruesse, E., Glöckner, F.O., Ludwig, W., Schleifer, K.-H., Whitman, W.B., Euzéby, J., Amann, R., Rosselló-Móra, R., 2014. Uniting the classification of cultured and uncultured bacteria and archaea using 16S rRNA gene sequences. Nat. Rev. Microbiol. 12 (9), 635.
Zhang, Q., De Clippeleir, H., Su, C., Al-Omari, A., Wett, B., Vlaeminck, S.E., Murthy, S., 2016. Deammonification for digester supernatant pretreated with thermal hydrolysis: overcoming inhibition through process optimization. Appl. Microbiol. Biotechnol. 100 (12), 5595–5606.
Zhang, Q., Vlaeminck, S.E., DeBarbadillo, C., Su, C., Al-Omari, A., Wett, B., Pümpel, T., Shaw, A., Chandran, K., Murthy, S., 2018. Supernatant organics from anaerobic digestion after thermal hydrolysis cause direct and/or diffusional activity loss for nitritation and anammox. Water Res.